PHOTONIC SENSORS / Vol. 7, No. 1, 2017: 20–26

Research on the Surface Subsidence Monitoring Technology Based on Fiber Bragg Grating Sensing

Jinyu WANG[1*], Long JIANG[2], Zengrong SUN[3], Binxin HU[1], Faxiang ZHANG[1], Guangdong SONG[1], Tongyu LIU[1,2], Junfeng QI[4], and Longping ZHANG[4]

[1]*Key Laboratory of Optical Fiber Sensing Technology of Shandong Province, Laser Institute of Shandong Academy of Science, Jinan, 250014, China*

[2]*Shandong Micro-Sensor Photonics Ltd, Jinan, 250014, China*

[3]*Shandong Shenglong Safe Technology Co. Ltd, Jinan, 250032, China*

[4]*Laiwu Mining Co. Ltd of Laiwu Steel Group, Laiwu, 271100, China*

[*]Corresponding author: Jinyu WANG E-mail: wangjinyu105@163.com

Abstract: In order to monitor the process of surface subsidence caused by mining in real time, we reported two types of fiber Bragg grating (FBG) based sensors. The principles of the FBG-based displacement sensor and the FBG-based micro-seismic sensor were described. The surface subsidence monitoring system based on the FBG sensing technology was designed. Some factual application of using these FBG-based sensors for subsidence monitoring in iron mines was presented.

Keywords: Fiber Bragg Grating; rock mass displacement; micro-seismic; optical fiber sensing; surface subsidence

Citation: Jinyu WANG, Long JIANG, Zengrong SUN, Binxin HU, Faxiang ZHANG, Guangdong SONG, *et al*., "Research on the Surface Subsidence Monitoring Technology Based on Fiber Bragg Grating Sensing," *Photonic Sensors*, 2017, 7(1): 20–26.

1. Introduction

Along with the continuous improvement of the mining technology and the application of large machinery, mining intensity and depth are increasing continuously; rock mass movement caused by mining has produced more and more serious impacts on the production and life, including endangering the life safety of miners and the safety of buildings on the ground, causing contradiction between workers and peasants, and even affecting the enterprise production. So the measurements of the rock mass displacement and the implementation of monitoring and early warning have become the necessary prerequisites for safe production and life.

The stability judgment of traditional field rock mass engineering is based on the observation of basic point of the ground surface displacement [1, 2]. The rock mass subsidence can be obtained by observing the basic point displacement. The basic point displacement is a result of rock movement, but not the movement process of rock mass. It plays an extremely important role in timely warning by monitoring deep rock mass deformation condition to keep safety. The optical fiber sensing technology has advantages such as high sensitivity, large dynamic range, and easy networking [3–5]. So it is possible to realize the high precision dynamic monitoring and

Received: 12 April 2016 / Revised: 27 August 2016

DOI: 10.1007/s13320-016-0331-y
Article type: Regular

early warning of rock mass shift by carrying out the rock displacement monitoring technology research based on the fiber optic displacement and seismic technology.

We designed two types of FBG (fiber Bragg grating)-based sensors. The principles of the FBG-based displacement sensor and the FBG-based micro-seismic sensor were described. We also proposed a surface subsidence monitoring system based on the FBG displacement and micro-seismic sensing technology. And some field test results in iron mine would also be presented.

2. Principles

2.1 FBG-based displacement sensor

According to the principle of fiber Bragg grating sensing [6], we designed a kind of FBG-based displacement sensor. The proposed FBG-based displacement sensor is shown in Fig. 1. The internal elastic element of the sensor is the strain beam with FBG1 pasted on the top and FBG2 pasted on the bottom. The wire-rope which is preloaded by the tension springs and connected to the telescopic slide will produce tensile changes caused by the subsidence, and then the strain beam which is close to the telescopic slides will move up and down, so the FBGs will subject to tensile stress and compressive stress.

The wavelength change of the FBG based on the co-production of temperature and strain can be expressed as

$$\Delta\lambda_B/\lambda_B=(\alpha+\zeta)\Delta T+(1-P_e)\varepsilon \qquad (1)$$

where α is the thermal expansion coefficient of the sensor, ζ is the thermo-optical coefficient of the optical fiber, P_e is the stress-optic coefficient, ΔT is the temperature difference, and ε is the axial strain of the fiber.

As two fibers are located in different surfaces of the cantilever beam, the strains of the two fibers are different. The wavelength changes of the two FBGs can be expressed as follows:

$$\Delta\lambda_{B1}/\lambda_{B1}=(\alpha+\zeta)\Delta T+(1-P_e)\varepsilon_1 \qquad (2)$$

$$\Delta\lambda_{B2}/\lambda_{B2}=(\alpha+\zeta)\Delta T+(1-P_e)\varepsilon_2 \qquad (3)$$

where λ_{B1} and λ_{B2} are the wavelengths of the FBGs. Subtracting (3) by (2), the strain difference can be given by

$$\varepsilon_1-\varepsilon_2=(\Delta\lambda_{B1}/\lambda_{B1}-\Delta\lambda_{B2}/\lambda_{B2})/(1-P_e). \qquad (4)$$

According to (4), the displacement and strain can be obtained without the influence of temperature.

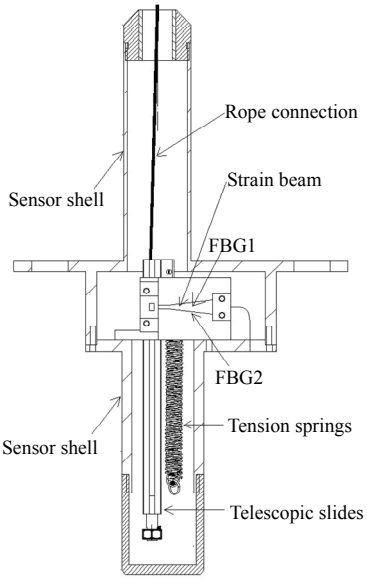

Fig. 1 Schematic of FBG-based displacement sensor.

2.2 FBG-based micro-seismic sensor

The schematic of the proposed FBG-based micro-seismic sensor as illustrated in Fig. 2 is composed of a steel leaf spring with the k_2 elastic coefficient, an L-shaped cantilever with an inert mass m connected to its end, and a fiber Bragg grating with the k_1 elastic coefficient with one end attached on the cantilever and another end attached on the shell. When the micro seismic waves induce vibration of the shell, the FBG will have a central wavelength shift due to the axial strain caused by the inertial force of the mass.

The dimensions a, b, and l are marked in Fig. 2.

The natural angular frequency can be defined as

$$\omega_0=\sqrt{k/m}=\sqrt{[k_2+k_1(a/b)^2]/m}. \qquad (5)$$

Assuming an external acceleration $a_g=A_g e^{i\omega t}$ and a relative damping coefficient δ, the strain

experienced by the FBG can be expressed as

$$\varepsilon = a \cdot a_g \Big/ b \cdot l \cdot \sqrt{(\omega_0^2 - \omega^2)^2 + 4\delta^2\omega^2} \ . \quad (6)$$

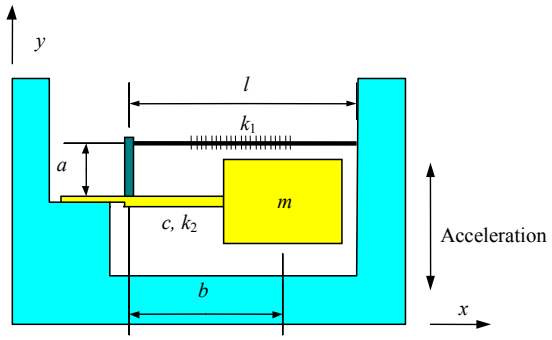

Fig. 2 Schematic of FBG-based micro-seismic sensor.

When the damping ratio $\zeta = \delta/\omega_0 = 0.7$, the strain acceleration sensitivity K can be noted as

$$K = a/bl\omega_0^2 \ . \quad (7)$$

The FBG wavelength shift is proportional to the strain experienced by the FBG. Considering the strain sensitivity for FBGs with peak wavelengths in the C band regime is about 1.2 pm/με in general, the accelerometer sensitivity (wavelength shift of FBG per unit acceleration) is given by

$$S = \Delta\lambda/a_g = 1.2 \cdot a/bl\omega_0^2 \ . \quad (8)$$

It can be seen from (5) and (8) that the natural angular frequency and the accelerometer sensitivity are determined by five parameters a, b, k_1, k_2, and m. By optimizing the parameters a, b, and m and choosing suitable material k_2, the micro-seismic sensor is designed to fit for micro-seismic measurement in mines. The frequency bandwidth is designed to be 1 Hz to 220 Hz, and the natural frequency is about 260 Hz according to the optimized parameters. The accelerometer sensitivity is 220 pm/g. Figure 3 shows the FBG-based micro-seismic sensor actually used in mine. Figure 4 shows the frequency response of the FBG-based micro-seismic sensor.

The interrogation principle of the FBG-based acceleration sensor depends on the intensity modulation of narrow line width DFB laser [7, 8], when a reflection or transmission spectrum curve of an FBG wavelength shifts due to the strain caused by vibration or acceleration.

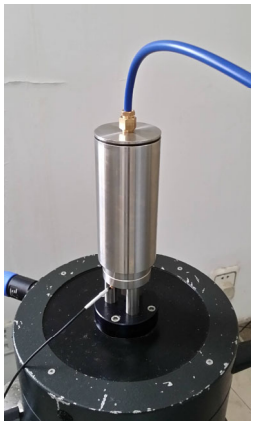

Fig. 3 Photograph of FBG-based micro-seismic sensor.

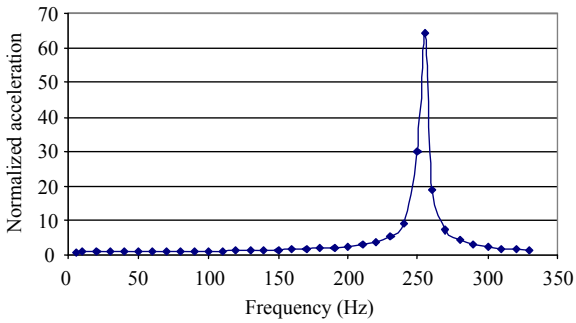

Fig. 4 Frequency response of the micro-seismic sensor.

3. Field test and results in iron mine

As the sinkhole of Zhao Zhuang iron mine once had a collapse, this monitoring system was established in iron mine in Zhaozhuang, Laiwu City, Shandong Province to protect nearby buildings, workers, and facilities. The surface subsidence monitoring system contains an FBG demodulator, an FBG micro-seismic demodulator, six FBG-based displacement sensors, four FBG-based acceleration sensors, and optical cables. The signals gathered by these sensors were transmitted to the host computer by cable in real time and analyzed by the software.

3.1 Displacement monitoring

On the ground with the electronic total station monitoring, there are 4 basis points. The positions of the basic points are shown in Fig. 5. Table 1 describes the sensors installation information. The shallow base of the FBG-based displacement sensors was all bellow 35 m.

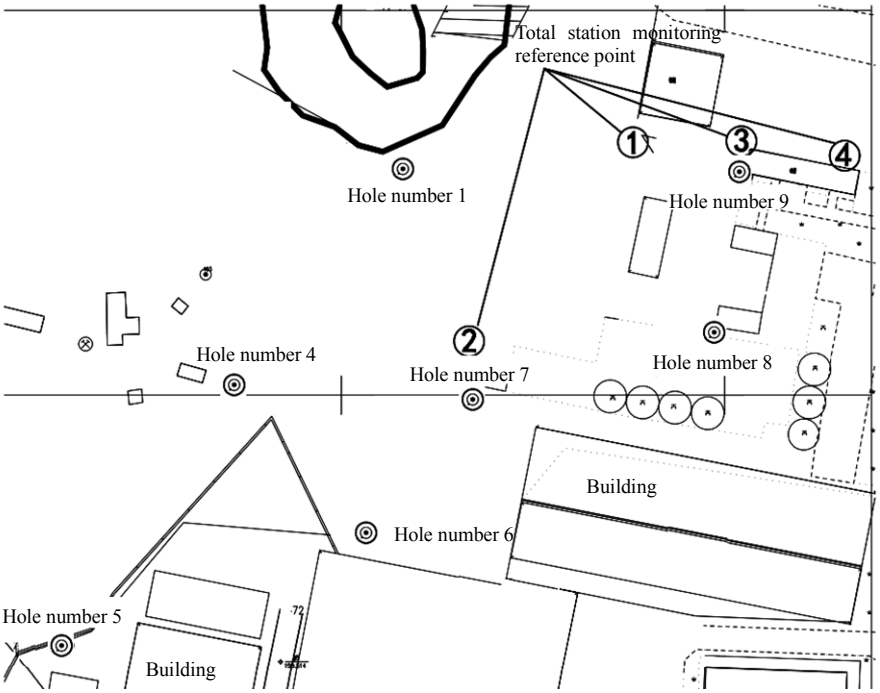

Fig. 5 Sensor installation plan.

Table 1 Placement information of displacement sensors.

Hole number	Sensor type	Installation depth (m)	Sensor number
6#	Shallow base	35	13K04A1001
	Deep base	56	13K04A2001
7#	Shallow base	40	13K04B1002
	Deep base	81	13K04B2002
8#	Shallow base	60	13K04A1002
	Deep base	69	13K04A2002

When the FBG-based displacement sensor is installed, it needs to be punched and drilled, and the sensor needs to be installed from the surface of the ground. Figure 6 shows the installation schematic diagram. The deep base, shallow point, and FBG-based displacement sensor are the fixed ends and connected through a connecting line. When there is a relative displacement among them, the FBG-based displacement sensor can detect these minor changes. If the deep base point and shallow point are placed in different rock strata, the changes between the strata of different depths can be monitored. Figure 7 shows the field installation of the FBG-based displacement sensor.

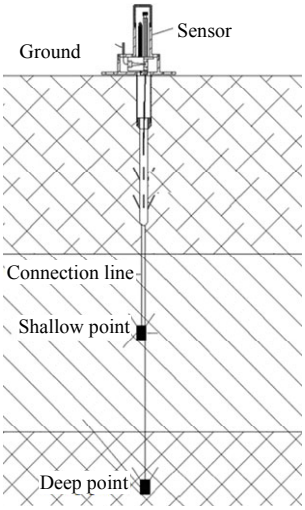

Fig. 6 FBG-based displacement monitoring installation design.

Fig. 7 Field installation of displacement sensor.

Figure 8 shows the displacement data from September 2014 to October 2015. Seen from Fig. 8, the cumulative deformation detected by the displacement sensor is more than 5 cm during this period. The results show that the surface subsidence tended to be stable between December 2014 and May 2015 except the data from Sensor 6. The cumulative data monitored by the deep base of Sensor 6 was reduced after April 2015. As the anchorage end of the sensor was affected by the local rock strata, if the rock at the anchoring part was damaged, the sensor here might fail to monitor. So a better and more reliable fixed way needs to be considered.

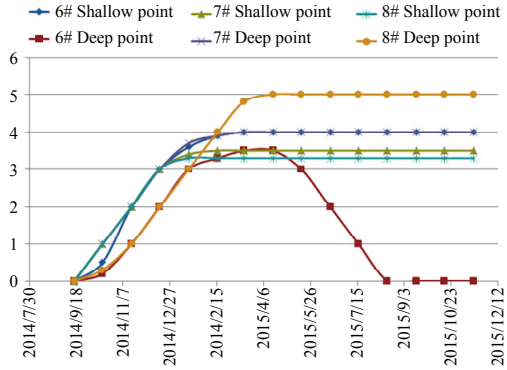

Fig. 8 Monitoring data of FBG-based displacement sensor.

Table 2 shows the displacement read from the electronic total station between June 2013 and December 2014. The average displacement is between 0.67 cm and 0.92 cm. Seen from the analysis result, the average subsidence rate got from the FBG-based displacement sensors is consistent with that obtained from the electronic total station.

Table 2 Statistics of monitoring data.

Hole number	Displacement (cm)	Average settlement (cm/month)
①	16.6	0.92
②	13.3	0.73
③	14.7	0.82
④	12	0.67

3.2 Micro-seismic monitoring

Table 3 describes the installation information of the FBG-based micro-seismic sensors. The FBG-based micro-seismic sensors were all installed bellow 55 m.

Figure 9 shows the field installation of micro-seismic sensors. The sensor was firmly installed on the bottom of the hole by special mounting rod. The grouting pipe, which was a kind of plastic hose and had 25-mm diameter, was inserted into the bottom of the hole. Expansion cements were grouted with manual injection pump, so the micro-seismic sensor could reliably coupled together with the strata. The principal component of expansion cement without shrinkage was Portland cement with the strength of 32.5, whose swelling agent rate was not less than 0.02%.

Table 3 Placement information of micro seismic sensors.

Hole number	Installation depth (m)	Sensor number
1#	60	13K05V1002
4#	84	13K05V1007
5#	62	13K05V1003
9#	55.5	13K05V1010

Fig. 9 Field installation of micro-seismic sensor.

Figure 10 shows the typical micro-seismic events occurred at 16:47:38 on December 27, 2014. The arrival time, energy, and location of the micro-seismic events could be obtained by analyzing the effective micro-seismic signals. Figure 11 shows the processing results of the micro-seismic events between September 2014 and December 2014. The dots and blocks represent different levels of micro-seismic events. represent different levels

of micro-seismic events. The block indicates the micro-seismic events that are larger than 10^5 J. And after January 2015, micro-seismic events happened rarely. This measurement result is consistent with the monitoring result of the displacement sensor. Combining these two kinds of detecting results, we can see that there is a strong rock activity.

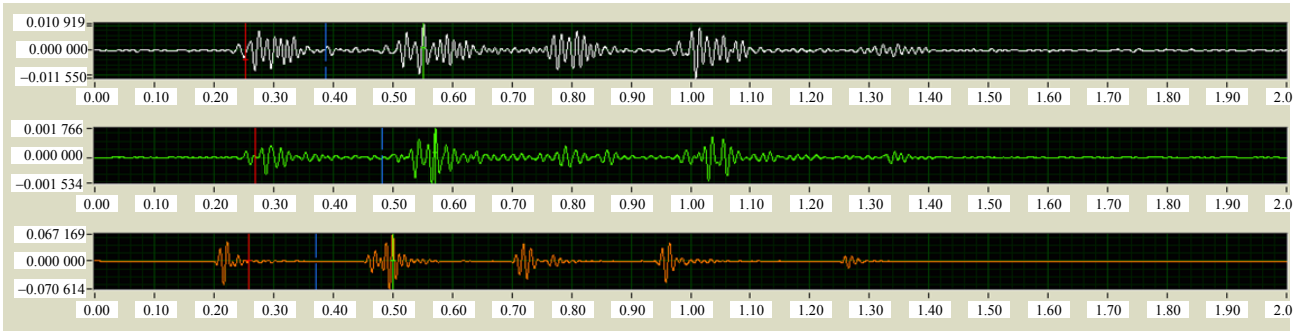

Fig. 10 Typical micro-seismic event.

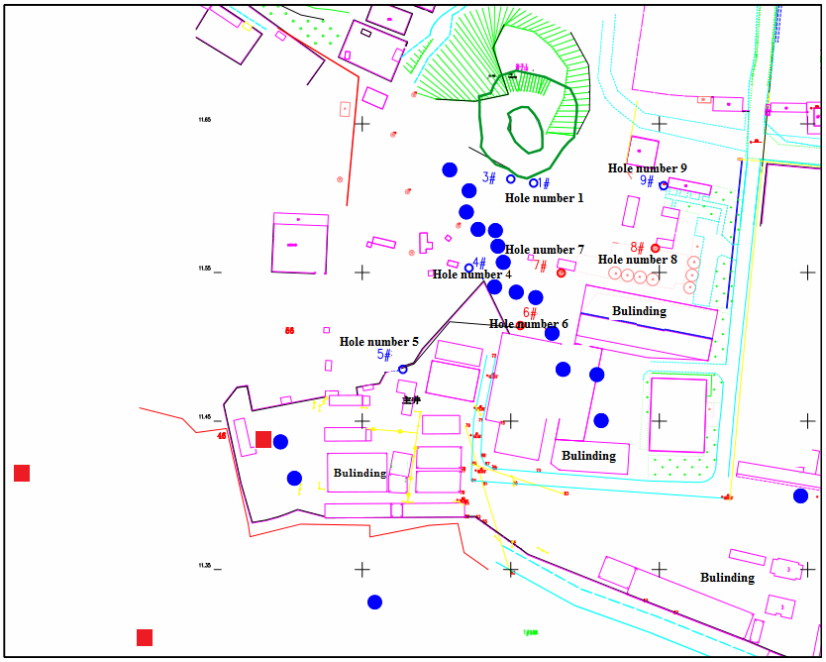

Fig. 11 Plane distribution of micro-seismic events.

4. Conclusions

In summary, we reported two types of FBG-based sensors to monitor the surface subsidence. The results show that the FBG-based displacement sensor and micro-seismic sensor can be combined to apply to the surface subsidence monitoring. The precision of the displacement result depends on the accuracy and reliability of the FBG-based displacement sensors, and the reliability of the analysis result of the micro-seismic events depends on the accuracy of the FBG-based micro-seismic sensor's coordinate, the location algorithm, the accuracy of first arrival, the installation location, the number of the micro-seismic sensor, and so on.

As the number of the micro-seismic sensors was too small, less effective micro-seismic events were obtained, and then the monitoring results needed further validation. In the future, we need to increase the measuring points to get more effective data to improve the monitoring accuracy. Then through the

feedback information, we can monitor damage occurring in a rock and progressive failure process much earlier and timely give the early warning of instability of rock mass.

Acknowledgment

This work was partly supported by the Science and Technology Development Plan of Shandong Province (No. 2014GSF120017) and Science Fund for Young Scholars of SDAS (No. 2013QN005). This work was also partly supported by the Development Funds for SMEs (part of the European cooperation) (No. SQ2013ZOC600005).

References

[1] X. U. Bigen, P. W. Chunlai, S. H. Tang, and P. L. Cheng, "Study on large goaf management and its monitoring scheme design," *China Safety Science Journal*, 2007, 17(12): 147–152.

[2] H. Wang, W. M. Yang, B. Wang, and C. Z. Zhao, "Judgment on surface subsidence danger of mine goaf based on GIS technology," *Coal Engineering*, 2008, 9: 119–123.

[3] J. Wu, V. Masek, and M. Cada, "The possible use of fiber Bragg grating based accelerometers for seismic measurements," in *Conference on Electrical and Computer Engineering*, Canada, pp. 860–863, 2009.

[4] A. D. Kersey, T. A. Berkoff, and W. W. Morey, "Multiplexed fiber Bragg grating strain sensor with a fiber Fabry-Perot wavelength filter," *Optics Letters*, 1993, 18(16): 1370–1372.

[5] J. G. Liu, C. Schmidt-Hattenberger, and G. Borm, "Dynamic strain measurement with a fiber Bragg grating sensor system," *Measurement*, 2002, 32(2): 151–161.

[6] K. O. Lee, K. S. Chiang, and Z. Chen, "Temperature-insensitive fiber-Bragg-grating-based vibration sensor," *Optical Engineering*, 2001, 40(11): 2582–2585.

[7] J. Y. Wang, T. Y. Liu, C. Wang, X. H. Liu, D. H. Huo, and J. Chang, "A micro-seismic fiber Bragg grating (FBG) sensor system based on distributed feedback laser," *Measurement Science and Technology*, 2010, 21(9): 094012.

[8] J. Wang, B. Hu, W. Li, G. Song, L. Jiang, and T. Liu, "Design and application of fiber Bragg grating (FBG) geophone for higher sensitivity and wider frequency range," *Measurement*, 2016, 79: 228–235.